Demonstration of Active Power Controls by Utility-Scale PV Power Plant in an Island Grid

Preprint

Vahan Gevorgian and Barbara O'Neill
National Renewable Energy Laboratory

Presented at the 15th International Workshop on Large-Scale Integration of Wind Power into Power Systems as well as on Transmission Networks for Offshore Wind Power Plants
Vienna, Austria
November 15–17, 2016

Conference Paper
NREL/CP-5D00-67255
February 2017

Contract No. DE-AC36-08GO28308

This report is available at no cost from the National Renewable Energy Laboratory (NREL) at www.nrel.gov/publications.

Available electronically at SciTech Connect http:/www.osti.gov/scitech

Available for a processing fee to U.S. Department of Energy and its contractors, in paper, from:

U.S. Department of Energy
Office of Scientific and Technical Information
P.O. Box 62
Oak Ridge, TN 37831-0062
OSTI http://www.osti.gov
Phone: 865.576.8401
Fax: 865.576.5728
Email: reports@osti.gov

Available for sale to the public, in paper, from:

U.S. Department of Commerce
National Technical Information Service
5301 Shawnee Road
Alexandria, VA 22312
NTIS http://www.ntis.gov
Phone: 800.553.6847 or 703.605.6000
Fax: 703.605.6900
Email: orders@ntis.gov

Cover Photos by Dennis Schroeder: (left to right) NREL 26173, NREL 18302, NREL 19758, NREL 29642, NREL 19795.

NREL prints on paper that contains recycled content.

Demonstration of Active Power Controls by Utility-Scale PV Power Plant in an Island Grid

Vahan Gevorgian, Barbara O'Neill
National Renewable Energy Laboratory (NREL)
Golden, CO, USA

Abstract—**The National Renewable Energy Laboratory, AES, and the Puerto Rico Electric Power Authority conducted a demonstration project on a utility-scale photovoltaic (PV) plant to test the viability of providing important ancillary services from this facility. As solar generation increases globally, there is a need for innovation and increased operational flexibility. A typical PV power plant consists of multiple power electronic inverters and can contribute to grid stability and reliability through sophisticated "grid-friendly" controls. In this way, it may mitigate the impact of its variability on the grid, and it can contribute to important system requirements more like traditional generators. In 2015, testing was completed on a 20-MW AES plant in Puerto Rico, and a large amount of test data was produced and analyzed that demonstrates the ability of PV power plants to provide various types of new grid-friendly controls. This data showed how active power controls can leverage PV's value from being simply an intermittent energy resource to providing additional ancillary services for an isolated island grid. Specifically, the tests conducted included the PV plant's participation in automatic generation control, the provision of droop response, and fast frequency response.**

Keywords-component; PV power plant; AGC; primary frequency response; fast frequency response

I. INTRODUCTION

Increasing solar generation coupled with increasing wind generation are displacing traditional power generation resources, specifically fossil-fueled thermal power plants. These conventional power plants are rotating machines that are synchronized to the electric grid, whereas wind and solar power plants are connected to the grid through an inverter (converting DC to AC energy), and therefore they are nonsynchronous to the grid's frequency.

Although utility-scale solar photovoltaic (PV) power plants are becoming a cost-effective energy resource, there is some concern that the increasing penetrations of PV technologies may potentially impact grid reliability. This is due to the variability across timescales and forecast uncertainty of the solar energy resource and impacts on both distribution and transmission systems [1], [2]. This may cause utilities to severely limit PV installations, curtail the output power, and/or increase assigned integration costs when considering a least-cost portfolio of resources. Deploying utility-scale, grid-friendly PV power plants that incorporate advanced capabilities to support grid stability and reliability is essential for the large-scale integration of PV generation into the electric grid [3], among other technical requirements, as a means to mitigate the impact of its variability on the power system. With the increased proportion of PV in the generation mix, the PV plant should be responsible for an increasing share of the grid's burden of reliability, stability, and high power quality.

A typical modern utility-scale PV power plant is a complex system of large PV arrays and multiple power electronic inverters, and it can contribute to grid stability and reliability through sophisticated grid-friendly controls. In 2012, the North American Electric Reliability Corporation's (NERC) Integration of Variable Generation Task Force made several recommendations on requirements for variable generators (including solar) to provide their share of grid support, including active power control (APC) capabilities [4], [5].

As an isolated island system, the Puerto Rico Electric Power Authority (PREPA) has a lower inertial constant compared to inertial constants of large interconnected power systems, such as on the mainland United States. During peak daytime hours when solar penetration is high and has displaced conventional generation, the available inertia from spinning mass is even lower because PV generation (unlike wind and conventional generation) does not have any rotating mechanical parts to replace inertia loss. With no stored kinetic energy available, a PV generation system has a very small time constant, i.e., a fast response to a step change in input on its circuit. This means that PV generators have a significant capability to participate in frequency support and, with additional control loops, to contribute to small-signal stability [6].

With this project's approach to holistic demonstration, the team sought to close existing gaps in perspectives by providing test data from a real, operating, utility-scale PV power plant to all stakeholders. If PV-generated power can offer a supportive product that benefits the power system and is economic for PV power plant owners and energy buyers, this functionality should be recognized and encouraged.

Note that this paper presents the summary of activities conducted by the National Renewable Energy Laboratory (NREL) in 2015 that are described in a higher level of detail in [7].

II. ACTIVE POWER CONTROLS BY PV POWER PLANTS

PREPA has a modern electric power system that serves the entire main island of Puerto Rico and its two adjacent islands of Vieques and Culebra. Currently, the total installed generation capacity in Puerto Rico is close to 6 GW, which includes 173 MW of wind and solar PV generation. The bulk of the electric generation in Puerto Rico is still largely based on petroleum and coal, with increasing participation by natural gas generators. Puerto Rico's transmission system consists of 230-kV and 115-kV lines as well as 38-kV subtransmission lines and 334 substations. PREPA's typical summer daytime peak load is approximately 2.8 GW.[1]

Based on the system needs, a PV power plant can provide APC to support reliability in a variety of ways. Generally, the forms of APC use adjustment of current output to aid in the reliability and security of the electric grid during certain situations [8]. For adjustments above the present operating point, reserve capacity, also known as headroom, is required; for adjustments below, it is not. For example, a generating unit somewhere on the system may have an unplanned outage, causing the generation and load on the system to be out of balance. This contingency disturbance event could be mitigated by a PV plant's APC adding power to the system if the PV plant has reserve capacity. Similarly, a contingency disturbance event could occur if a large load is disconnected from the system, leaving a surplus of generated power. In this case, a PV plant's APC could be curtailed to decrease system power. The latter scenario is less common, so generally we focus on the former.

AES's 20-MW Ilumina PV power plant is located in Guayama, Puerto Rico, and has been operating commercially since 2012. An aerial photo of the plant is shown in Figure 1. Forty inverters (rated for 500 kWac) from Green Power Technologies Corporation (GPTech) were incorporated in 20 integrated arrangements of 1 MW. The plant is connected to PREPA's grid at the point of interconnection via a 20-MVA step-up 13.2/38-kV transformer.

Figure 1. Aerial view of AES Ilumina PV power plant

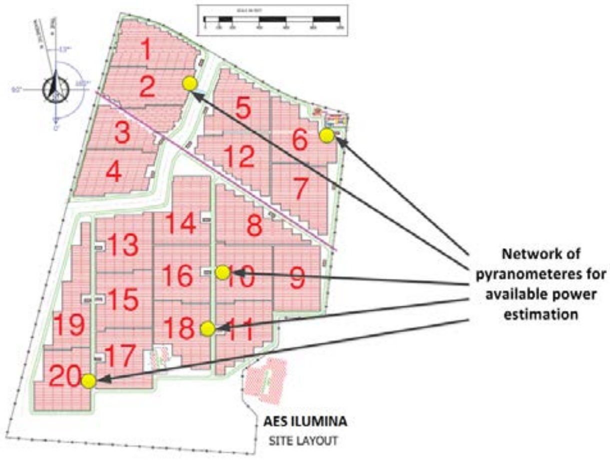

Figure 2. Plant layout (courtesy of AES)

III. Testing AGC Participation by Ilumina PV Plant

The Ilumina plant has pyranometers that have been installed to measure solar irradiance as well as solar radiation flux density. The power plant controller (PPC) has the function of estimating the available peak plant power utilizing those solar irradiance measurements (Figure 1). The plant is divided into five control sectors with individual pyranometers located in each sector. The available power in each sector is estimated by the controller using the following equation:

$$P_{sector} = Irr \times W_{sector} \times \left(\frac{N_{available}}{N_{total}}\right) \times Scale + Offset \qquad (1)$$

where Irr is the measured solar irradiance (Watt/m^2); $Weight_{sector}$ is the weight of the sector compared to the plant capacity; $N_{available}$ and N_{total} are the number of available and total number of inverters, respectively; and $Scale$ and $Offset$ are unit conversion factors.

The estimated total available peak plant power is then calculated every 0.5 s as:

$$P_{plant} = \sum_{k=1}^{5} P_{sector,k} \qquad (2)$$

This method of calculating peak plant power is based only on irradiance and does not include other parameters that may significantly impact the accuracy of the estimation. In particular, the effect of panel temperatures on plant efficiency is not considered by this method. Other parameters, such as inverter efficiency variations at different load levels, are also important for accurately estimating available power. In addition, dust accumulation on panels caused by various external factors (e.g., nearby traffic and other industrial activities) will also impact the accuracy of the method used to estimate Ilumina's available power. The PPC estimation of available plant power was relatively simplistic for purposes of these tests and hypothetically could be refined to consider the nonlinear factors mentioned above, if necessary.

The purpose of automatic generation control (AGC) control is to enable the PV power plant to follow the active power set

[1] Puerto Rico's load has decreased since its historic peak in 2005 of 3.685 MW.

point sent by PREPA's AGC system. The set-point signal is received by PREPA's remote terminal unit (RTU) at the plant substation and then scaled and routed to the PPC via real-time automation controller (RTAC) and SmartBridge, as shown in Figure 2. In the same time frame, the values of both the plant's actual power and available peak power are calculated in accordance with (2) and are sent back to PREPA's AGC system.

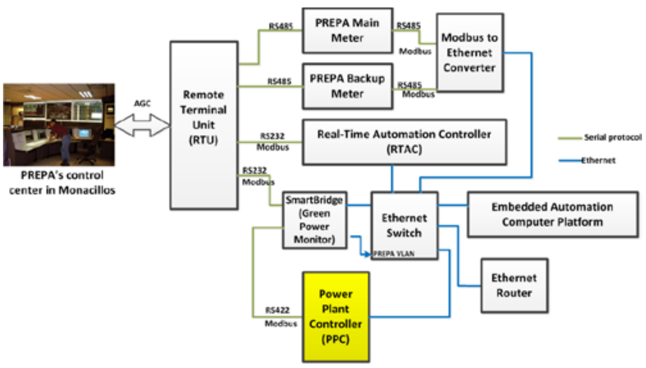

Figure 3. Diagram of AES PV plant's communications

For purposes of these tests, when in AGC mode, the PPC initially set the plant to operate at a power level that was 10% lower than the estimated available peak power to have headroom for following the up-regulation AGC signal. The lower boundary of AGC operation can be set at any level below the available peak power, including full curtailment, if necessary. After testing the AGC with 10% curtailment, NREL experimented with 20% and 40% curtailment. Even lower levels of operation and full curtailment are possible, but they were never tested to reduce the impact on plant revenues and the cost of the demonstration.

PREPA's AGC was set to send a direct set-point signal in the range from 1–20 MW with the step change of 0.05 MW. Thus, a 50-kW AGC set-point resolution was achieved on this 20-MW PV power plant. PREPA defined the plant in its AGC database by masking it under the identifier of another conventional unit. All ramp-rate settings in the PV power plant PPC were supposed to be disabled during the AGC tests. AGC control logic for a single-area power system with no interconnections (such as PREPA) is based on determining the:

- Island's total desired generation
- Base points for each AGC participating unit
- Regulation obligation for each AGC participating unit.

Area control error (ACE) is an important factor used in AGC control. For an island system, ACE is determined as:

$$ACE = -10B(f_a - f_s) + I_{ME} + I_T \qquad (3)$$

where B is the frequency bias (MW/0.1 Hz); f_a and f_s are the actual measured and scheduled (60-Hz) frequencies, respectively; and I_{ME} and I_T are the meter error correction and time error correction factors, respectively (MW). The ACE value is then used by the AGC control logic to determine the total desired generation that will drive it to zero. The desired generation for each participating generating unit is split into two components: the base point and regulation. The base point for each generating unit is set at its economic dispatch point, and the island's total regulation is calculated as the difference between the total desired generation and the sum of the base points for all AGC participating units. The total regulation for the whole system is allocated among all participating regulating units. Ilumina is considered one plant-level generating unit, and individual inverter outputs are not considered by PREPA's operations. Various unit-specific parameters are used in its regulation allocation, such as ramp rates and operating limits. Figure 4 shows a snapshot of the portion of PREPA's AGC control display when a 19-MW set point was sent to the AES's Ilumina RTU.

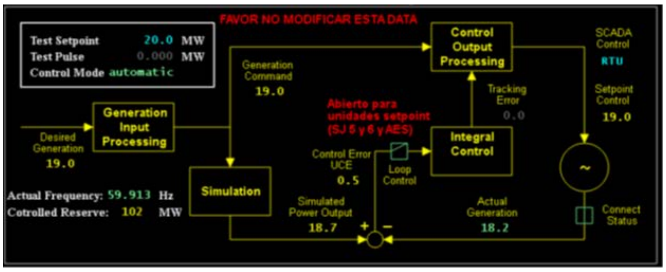

Figure 4. Diagram of PREPA's unit control (image from PREPA)

IV. AGC TEST RESULTS

AGC tests were conducted in August 2015. During these, the plant was set to participate in AGC control, and it was allowed to operate within power ranges of 20% and 40% below estimated available peak power. During this testing period, the plant demonstrated good AGC performance, as shown in Figure 5 and Figure 6 for the 20% and 40% cases, respectively, which represent the time series of the measured plant power, grid frequency, AGC set point received from the PREPA energy control center, and the estimated peak and curtailed power levels. The correlation between measured power and the AGC set point for each test is shown in Figure 7 and Figure 8. During periods of rapid PV power plant production decline due to cloud movement (e.g., the time period between 15:23 and 15:34 in Figure **5**), the plant was not able to follow the AGC signal with the same level of precision as it was during periods of low power variability.

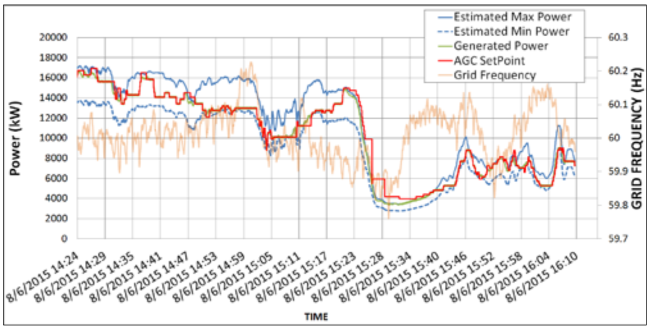

Figure 5. AGC test using 20% range

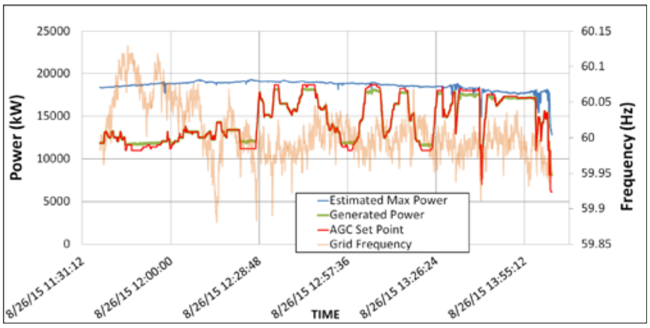

Figure 6. AGC test using 40% range

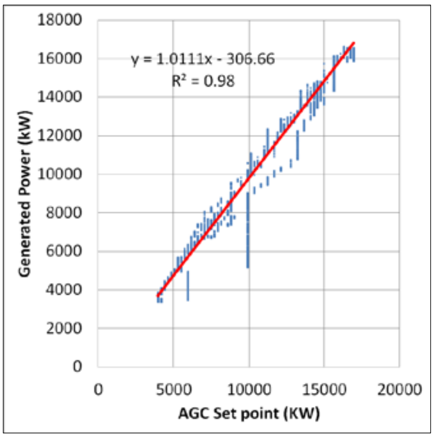

Figure 7. Correlation between AGC set point and measured power for 20% case

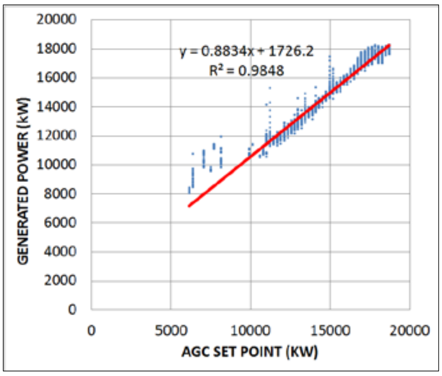

Figure 8. Correlation between AGC set point and measured power for 40% case

A closer look at the test data also revealed time periods of smooth power production when the plant was not able to reach the set point. A more detailed explanation of this mismatch between set point and actual plant output is shown in Figure 9. Two types of mismatch can be observed in Figure 9 from the August 14 data. The first type took place when the AGC set point was close to the value of the estimated plant peak power. The AGC system assumed that there was still some available headroom for up-regulation because its evaluation was based on the available plant power value that was communicated by the plant PPC. However, as mentioned in Section III, estimating available peak power based only on pyranometer measurements is subject to uncertainties because some other important parameters are not considered. As a result, the calculated available power was overly optimistic, and the inverters were not able to produce as much power because they were already operating at their maximum peak power point. Therefore, the control error appeared every time the AGC set point was above the actual peak power of the plant, as shown in Figure 9. As mentioned in Section III, these uncertainties, and hence a source of control error, could be minimized if the plant's available power were better modeled by incorporating significant variables into the calculation, such as panel productivity based on ambient temperature, inverter efficiency, and environmental dust of available power. For this test, NREL did not require GPTech to model this calculation as precisely as would be possible given more time and financial incentive to obtain an accurate estimation.

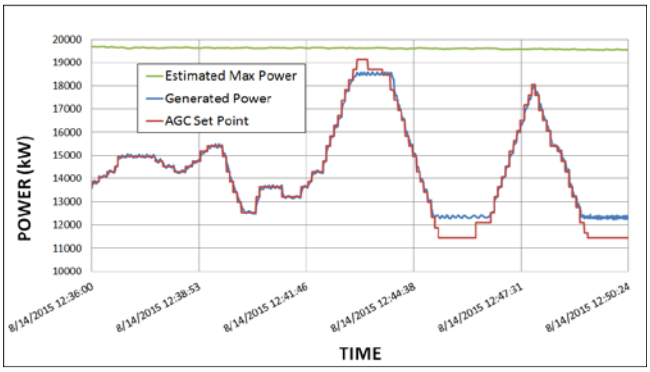

Figure 9. AGC performance explained

Another source of mismatch between the set point and actual plant power appeared during times when AGC requested less power than the 40% lower limit. Note that this limit was "artificial," and it was set to minimize revenue losses to AES. The plant is fully capable of further curtailing its production in accordance with an AGC order.

It is remarkable that during a significant amount of time, AES's Ilumina PV power plant was the only resource in PREPA participating in AGC. Such periods took place during all four days of AGC testing when the load variations in PREPA's system were small. Other plants were requested to participate in AGC when the contribution from AES's Ilumina was not sufficient to balance the frequency.

V. FREQUENCY DROOP TESTS

The definition of implemented droop control for PV is the same as that for conventional generators:

$$Droop = \frac{\Delta P / P_{rated}}{\Delta f / 60Hz} \qquad (4)$$

Plant rated power (20 MW) is used in (4) for the droop-setting calculations. For the droop test, the plant was set to operate at a curtailed power level that was 10% lower than the available estimated peak power. The PPC was programmed to change the power output of the plant in accordance with a symmetric droop characteristic, shown in Figure 10, at both 5% and 3% droop value. The upper limit of the droop curve was the available plant power, and the lower limit was at a level that was 20% below the then-available peak power, or 10% below the operated power level, to minimize revenue losses. The implemented droop curve also had a ±12-mHz frequency dead band.

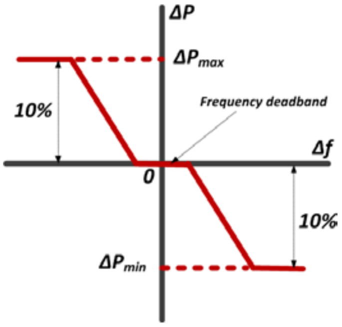

Figure 10. PV plant's droop characteristic

The 5% and 3% frequency droop tests on AES's Ilumina PV power plant were conducted during many hours in August 2015. For this purpose, before beginning each test, the plant controller was set to droop mode with 5% or 3% droop value and 10% power curtailment. The minimum allowed power level for down-regulation was set at 20% below available power for all droop tests (to minimize plant revenue losses). Also, a 25-mHz frequency dead band was used in the droop characteristic for all tests. The results of one 3% droop test are shown in Figure 11, which includes the recorded time series of actual plant power, estimated peak power, and grid frequency. The plant controller forced the plant power to follow the grid frequency in accordance with the 3% droop. The droop response of the plant is more visible if the change in power (*ΔP*) and change in frequency (*Δf*) are shown instead of absolute values, as in Figure 12.

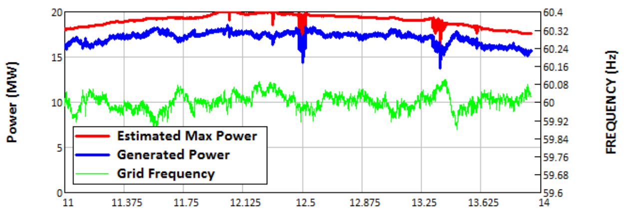

Figure 11. Measured times series for 3% droop test

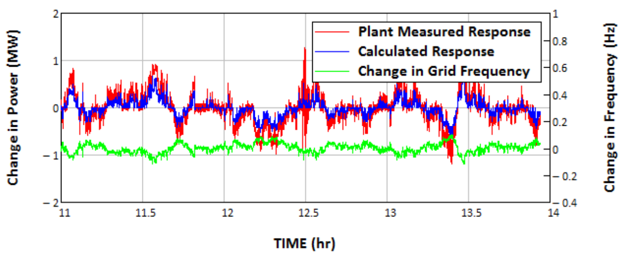

Figure 12. Change in frequency and power for 3% droop test

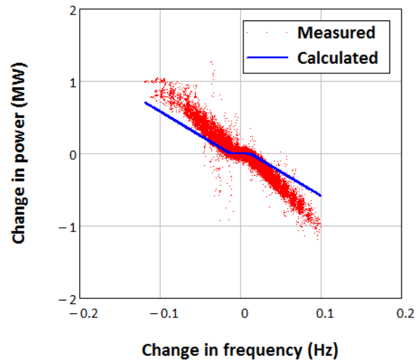

Figure 13. Measured droop characteristic

Figure 13 shows the calculated actual measured and calculated plant *ΔP* that corresponds to frequency deviation, *Δf*. The following equations were used to calculate the values:

$$\Delta f = f_{measured} - 60Hz \qquad (5)$$

$$\Delta P_{measured} = P_{actual} - P_{max.estimated} \qquad (6)$$

$$\Delta P_{measured} = P_{actual} - P_{max.estimated} \qquad (7)$$

where $f_{measured}$ is the actual grid frequency as measured on the plant terminals, $\Delta P_{calculated}$ is the ideal (or target) response of the plant to grid frequency variations for a given droop setting, and P_{nom} is the plant's nameplate capacity (20 MW).

The distribution of control error during the 3% test is shown in Figure 14. The maximum and minimum absolute error is around 1 MW with mean error close to zero MW.

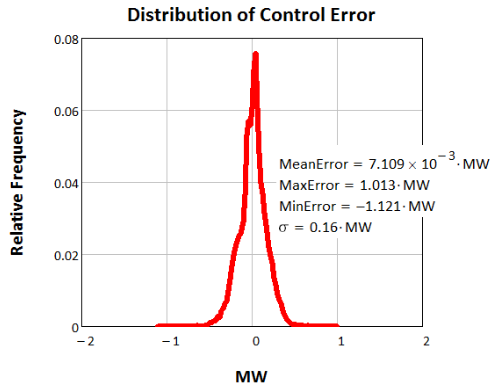

Figure 14. Control error during 3% droop tests

The results of the tests for both 5% and the more aggressive 3% droop cases were consolidated and are shown in Figure 15. The measured data points were plotted against calculated ideal droop response for both cases. The grid frequency actual deviations during both tests were generally within a range of ±0.1 Hz, so it was not possible to test the plant's performance during larger frequency fluctuations.

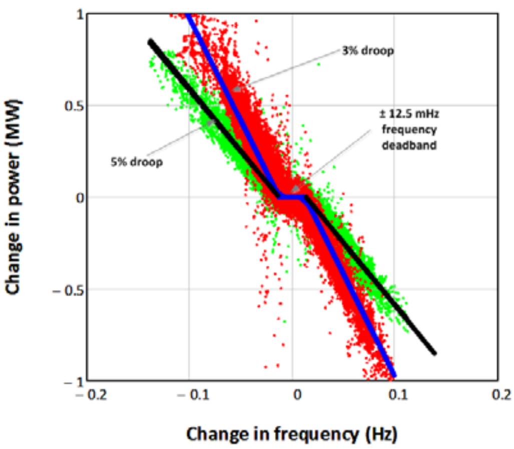

Figure 15. Results for 3% and 5 % droop tests

VI. Fast Frequency Response Tests

The fast frequency response (FFR) by the PV plant is intended to supplement the inherent inertial response from synchronous machines and synthetic inertial response from inverter-coupled wind generation. One Electric Reliability Council of Texas (ERCOT) analysis suggests that under certain conditions, the impact of 1 MW of FFR on the overall system frequency response is equivalent to 2.35 MW of primary frequency response [9]. Although FFR by PV power plants cannot completely replace inertia, it can help reduce the initial rate of change of frequency (ROCOF). FFR is a response that needs to be deployed automatically and provide a full response as fast as possible after the frequency drops below a preset threshold, e.g., within 0.5 s, according to the proposed FFR requirement in ERCOT's ancillary service market design [10].

FFR tests were conducted at AES's Ilumina plant with a 10% curtailment set point. FFR was triggered by providing a step-change control signal to the PPC, simulating a condition of rapid frequency drop. The plant controller was programmed to deploy its curtailed reserve as fast as possible (within 500 ms) in response to this simulated frequency event. The test was repeated many times during three different production levels: high, medium, and low power.

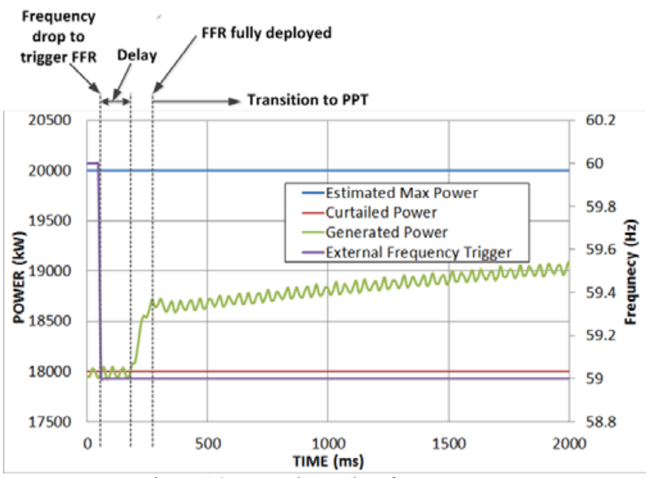

Figure 16. Example results of one FFR test

The test demonstrated that the plant essentially deployed all its available reserve within 500 ms from the beginning of the event at any power level. One example of the test results at high power level is shown in Figure 16. The FFR was triggered by the external underfrequency signal after a short 100-ms delay. The plant was able to deploy its reserves within another 100 ms. Upon completion of the FFR deployment, the peak power tracking (PPT) algorithm took over to drive the plant output to its maximum available power. Similar FFR tests were conducted at high, medium, and low power levels, and all demonstrated the plant's ability to provide FFR within the required response speed limits.

VII. Conclusions

The focus of this project was on demonstrating the controls of utility-scale PV power plants to provide various types of active and reactive power controls for ancillary services. Active power control capabilities for inverter-connected plants such as PV power plants have been acknowledged and available for a number of years; however, many of these capabilities have not been proven in a real, commercially operational setting by interfacing with the plant operator on the ground as well as the system operator (either utility off-taker or transmission system operator).

This project, funded through the U.S. Department of Energy (DOE), Solar Energy Technologies Office, gained valuable real experience for all industry players with (1) the PV power plants' implementations of these capabilities, (2) the system operators' communications acceptance of the signals and use of the signals, (3) the iterative loop for the system operators to send back appropriate information (i.e., set point), (4) the logic of the PV power plant controllers to respond to the set points, and (5) the PV power plants' return of more up-to-date information (i.e., plant capability) to complete the iterative loop. This test is the first step in implementation; further refinements will take place as more data and experience are available to improve the proposed concept.

Acknowledgments

The authors thank the DOE Solar Energy Technologies Office for supporting this work. We acknowledge the substantial contributions to this report provided by staff at the Puerto Rico Electric Power Authority (PREPA). We also thank AES and GPTech for their collaboration in the project. This work was supported by DOE under Contract No. DE-AC36-08GO28308 with NREL. Funding provided by DOE SETO.

References

1. M. Lave, J. Kleissl, A. Ellis, and F. Mejia, "Simulated PV power plant variability impact of utility-imposed ramp limitations in Puerto Rico," in IEEE 2013 PV Specialists Conference Proceedings. Piscataway, NJ: Institute of Electrical and Electronics Engineers, 2013.
2. E. Ela, V. Diakov, E. Ibanez, and M. Heaney. Impacts of Variability and Uncertainty of Solar Photovoltaic Generation at Multiple Timescales (NREL/TP-5500-58274). Golden, CO: National Renewable Energy Laboratory, May 2013. Accessed September 17, 2014: http://www.nrel.gov/docs/fy13osti/58274.pdf.
3. M. Morjaria, D. Anichkov, V. Chadliev, and S. Soni, "A grid-friendly plant," IEEE Power and Energy Magazine, May/June 2014.

4. North American Electric Reliability Corporation, Integration of Variable Generation Task Force Report. Washington, DC: 2012.

5. A. Ellis, R. Nelson, E. Engeln, R. Walling, J. McDowell, L. Casey, E. Seymour, W. Peter, C. Baker, and B. Kirby, Reactive Power Interconnection Requirements for PV and Wind Plants: Recommendations to NERC (SAND2012-1098). Albuquerque, NM: Sandia National Laboratories, February 2012.

6. Y. Liu, J. Garcia, and S. Hadley, Wind/PV Generation for Frequency Regulation and Oscillation Damping in the Eastern Interconnection (EI) (ORNL/TM-2013/587). Oak Ridge, TN: Oak Ridge National Laboratory, December 2013. Accessed September 17, 2014: http://info.ornl.gov/sites/publications/files/Pub47594.pdf.

7. V. Gevorgian and B. O'Neill, Advanced Grid-Friendly Controls Demonstration project for Utility-Scale PV Power Plants (NREL/TP-5D00-65368). Golden, CO: National Renewable Energy Laboratory, January 2016. www.nrel.gov/docs/fy16osti/65368.pdf.

8. E. Ela, V. Gevorgian, P. Fleming, Y. C. Zhang, M. Singh, E. Muljadi, A. Scholbrook, J. Aho, A. Buckspan, L. Pao, J. Singhvi, A. Tuohy, P. Pourbeik, D. Brooks, and N. Bhatt, Active Power Control from Wind Power: Bridging the Gaps (NREL/TP-5D00-60574). Golden, CO: National Renewable Energy Laboratory, January 2014. Accessed September 17, 2014: http://www.nrel.gov/docs/fy14osti/60574.pdf.

9. J. Matevosyan, "Future ancillary services development in ERCOT" (presentation given at the IEEE Power and Energy Society General Meeting, Piscataway, NJ, 2014).

10. ERCOT, "Future ancillary services in ERCOT: Concept paper, Ver. 1.0. Austin, TX: April 2014. http://www.ferc.gov/CalendarFiles/20140421084800-ERCOT-ConceptPaper.pdf